

Simulation of Nanopattern Formation of Si Surface due to Ion Irradiation



Sarwar H. Ali*, S. R. Saeed**

* Department of Physics ,Faculty of Science and Educational Science, Sulaimani, Kurdistan region, Iraq, sarwar.hasan77@yahoo.com

** Department of General Science, Faculty Education - Chamchamal, University of Sulaimani, Chamchamal, Kurdistan region, Iraq, salah.saeed@univsul.net.

Received: 25 Nov. 2013, Revised: 17 Dec. 2013, Accepted : 27 Jan. 2014

Published online: 26 Mar. 2014

Abstract:

Energetic ion irradiation induce surface nano-scale patterns formation, ripple or wavelike pattern is one of the surface morphologies. Analytical solution of the BH continuum equation, using MATLAB applied on Si target, well-defined ripple structure were observed as a function of different parameters such as angle of ion incidence, ion energy, ion flux, ion species, and thermal diffusion coefficient

Keywords: ion irradiation; Bradley-Harper theory; surface nanopattern.

Introduction:

Sputtering is the removal of material from the surface of solids through the impact of energetic particles [1]. The sputtering phenomenon, which is caused by the target surface by particle bombardment, was first noted by Grove in a dc gas discharge tube in 1852 [2]. The evolution of the surface morphology during ion sputtering is a complex phenomenon involving roughening and smoothing processes.

Depending on the properties of the substrates that eroded and the erosion conditions, it is even able to create some surprisingly ordered submicron/nanoscale features like dots [3] holes [4] nanowires [5] and ripples on the surface [6]. It is believed that ripples are produced as a result of the interplay between a roughening process caused by the erosion (sputtering) of the surface by ion energy dissipation at the subsurface region, and a smoothing process by thermal or ion induced

diffusion driven by reducing surface energy. [7]

Several theoretical models has set to explain the evolution of the topography under ion sputtering. A particularly successful model has been proposed by Bradley and Harper (BH) [8] they proposed a linear continuum equation by combining Sigmund's model of ion-beam erosion with diffusion theory. However, certain experimentally observed features, such as the saturation of the ripple amplitude and the appearance of kinetic roughening, are not predicted by the linear BH theory [9]. Initially the BH equation was extended to a non-linear equation [10], and then it was modified to an equation of the Kuramoto-Shivashinsky (KS) type [11] and to the anisotropic KS equation [12]. Finally by coupling KS equation with hydrodynamic model it was possible to reproduce pattern coarsening [13]. It is mandatory to mention that all the models are rooted in the famous Sigmund theory of sputtering [14] established

9 years after the first experiment of the ripple formation. Sigmund theory assumes that the local erosion rate is proportional to the intersection of the surface with a three-dimensional Gaussian distribution of energy deposited by a collision cascade [15].

Generally, ripples are typically oriented perpendicular to the incident ion beam projection in the surface plane for small angles of incidence (relative to the surface normal), whereas for large angles the observed ripple is rotated by 90° [16]. The variation of ripple wave length with ion energy [17], ion species [18], flux [19], thermal diffusion coefficient [20] have been reported.

Bradley and Harper Model (BH model)

A. Theory of Ripple Formation

The ion sputtering with low and medium energy and off-normal incident ion produce a self-organized process at the irradiated surface which leads to the formation of wavelike or ripple structures in the submicron range.

In 1988, based on the Sigmund theory of sputtering, Bradley and Harper (BH) proposed a linear continuum equation to explain the main features of ripple formation on amorphous materials under ion bombardment [8]. The curvature dependence of the erosion rate produces an instability of the surface against periodic disturbances that causes an amplification of the initial roughness spectrum [21], i.e. the amplification of a surface modification is due to the difference between the local sputtering yields, higher at the bottom of the valleys, lower at top of the hills [22].

The linear continuum equation, BH model, describes the surface topography evolution combines the curvature dependent sputtering with surface smoothing via thermally activated surface diffusion:

$$\frac{\partial h}{\partial t} \cong -v_0(\theta) + v'_0(\theta) \frac{\partial y}{\partial x} + \frac{Ja}{N} Y_0(\theta) \left[\Gamma_x(\theta) \frac{\partial^2 h}{\partial x^2} + \Gamma_y(\theta) \frac{\partial^2 h}{\partial y^2} \right] - B \nabla^2 \nabla^2 h \quad (1)$$

where h is the height of the surface according to the average height, v_0 is the erosion velocity of a flat surface, v'_0 is the velocity of the perturbed surface, J is the ion flux, a is the average depth of energy deposition, N is the number of atoms per unit volume in the amorphous solid, $\Gamma_{x,y}$ is the effective surface tension coefficient in x and y directions, x is defined as the spatial coordinate parallel to the projected direction of the ion beam on the plane of average surface orientation and y is the coordinate within this plane normal to x .

The first term on the right hand side of equation (1) represents the erosion rate of the flat surface, the second one the lateral movement of the structures on the surface, the third term represents the curvature dependent sputtering and the last term the surface diffusion. B is the thermally diffusion coefficient (in the case of the thermally activated diffusion), and Γ_x and Γ_y are the coefficients that describe geometrical distribution of the deposited energy [8]. And the thermally activated diffusion coefficient is given by:

$$B = \frac{D_s q \delta}{N^2 k_B T} \quad (2)$$

where D_s is the surface self-diffusivity, q is the surface free energy per unit area, δ is the areal density of diffusing (surface) atom, k_B is the Boltzmann constant and T is the absolute temperature.

BH equation can be rewrite with Makeev expression as [12]:

$$\frac{\partial h}{\partial t} = -v_0 + \gamma \frac{\partial h}{\partial x} + v_x \frac{\partial^2 h}{\partial x^2} + v_y \frac{\partial^2 h}{\partial y^2} - B \nabla^4 h \quad (3)$$

Here, v_o is the erosion velocity of the planar or flat surface. This term does not affect the ripple features, such as ripple wavelength and ripple amplitude. The coefficient γ contributes only to the velocity of the ripples along the x direction (i.e. it causes a lateral movement of the structures), leaving unaffected the y component of the ripple velocity. Thus, as expected, $\gamma = 0$ for normal incidence ($\theta = 0$). γ does not affect the ripple characteristics also. v_x and v_y are the effective surface tension produced by the erosion process, dependent on the ions incidence angle, θ , they are the origin of the instability responsible for ripple formation. Consequently, they play a particularly important role in determining the surface morphology. The sign and the magnitude of v_x and v_y determine both the wavelength and the orientation of the ripples [12].

B. Ripple Orientation and Wavelength

In BH continuum equation the ripples orientation is determined by the coefficient Γ_x or Γ_y having minimum values [8]. It is observed that Γ_x has negative or positive value depending on the incidence angle, while Γ_y is always negative. At normal incidence, where $\Gamma_x = \Gamma_y$, ripple orientation is not observed; depressions or hills may evolve, probably as a result of the waves with different directions. At off-normal incidence and up to the critical angle θ_c , it is observed that $\Gamma_x < \Gamma_y$, thus the ripples are perpendicular to the ion beam projection on the surface. For larger incidence angles, where $\Gamma_x > \Gamma_y$ the ripples are parallel to the ion beam direction.

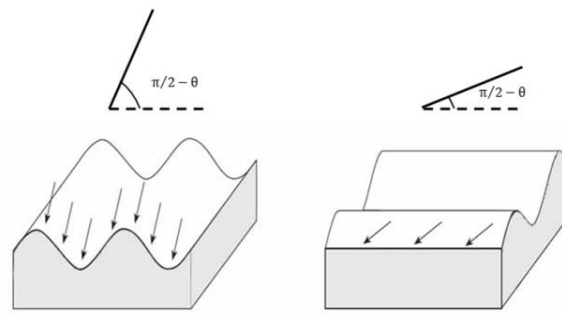


Fig. (1) Dependence of the ripple orientation on the ion incidence angle, θ ; (a) orientation for small θ and (b) orientation for an angle close to $\pi/2$.

Any perturbation of the planar surface at $t = 0$ can be written as a superposition of periodic height modulations. For a short time each of the contributors (in the 1st four contributors of equation 1) contributes to $h(x, y, t)$ independently. The exponential growth of the height $h(x, y, t)$ of the ripple structure may be assume as:

$$h(x, y, t) = -v_o(\theta)t + h(x, y, 0) \exp(-i(k_x x + k_y y - \omega t) + r_g t) \quad (4)$$

putting this equation in equation (1), angular frequency ω and the growth parameter r_g (with real values of k_x, k_y, ω and r_g) become:

$$\omega = -v'_o(\theta)k_x \quad (5)$$

$$r_g = -\frac{I_a}{N} Y_0(\theta, E) [\Gamma_x(\theta)k_x^2 + \Gamma_y(\theta)k_y^2] - B(k_x^2 + k_y^2)^2 \quad (6)$$

Where E is the incident ion energy and $k_{x,y}$ is the wave numbers in the direction of x and y . Generally, the growth parameter r_g takes the form:

$$r_g = -\frac{I_a}{N} Y_0(\theta, E) [|\Gamma_i(\theta)|k_i^2 - Bk_i^4] \quad (7)$$

where $\Gamma_i(\theta) = \min[\Gamma_x(\theta), \Gamma_y(\theta)]$, the wave vector $k_i (= \frac{2\pi}{\lambda_i})$ observed exponentially is that

which has the largest value of r_g and gives the ripple wavelength as:

$$\lambda_i(\theta, E) = 2\pi \left(\frac{2NB}{J\alpha Y_0(\theta) |\Gamma_i(\theta)|} \right)^{1/2} \quad (8)$$

According to equations (2) and (8), at high temperatures and low fluxes the wavelength varies as ($\lambda \sim (JT)^{-1/2} \exp(-\Delta E/2k_B T)$), where k_B is the Boltzmann's constant, T is the substrate temperature and ΔE is the activation energy for surface self-diffusion. and

$$\lambda \sim \frac{1}{E^{1/2}} \quad (9)$$

In the BH model, the redeposition and reflection are not taken into account. Thus, the model is valid only for small amplitude features and incidence angles smaller than that for which the sputter yield is maximal. In general BH model successfully predict some experimental observations such as ripples orientation, as well as the exponential growth of the amplitude at short times [23].

Analytical solution of ripple orientation and wavelength according to BH model

To show the induced ripples pattern due to the ion irradiation on the Si surface and their wavelengths dependence on some parameters, equations (4-6, 8) are used in the analytical solution by MATLAB program for BH continuum equation, but in Makaevev *et al.* expression [12]. The general solution of equation (3) used in the analytical solution:

$$h = -v_0(\theta)t + h_0 e^{(r_g - i\omega)t} \quad (10)$$

here

$$\omega = -\gamma k_x \quad (11)$$

and

$$r_g = -(v_x k_x^2 + v_y k_y^2) - B (k_x^2 + k_y^2)^2 \quad (12)$$

The wavelength of the induced ripples given by:

$$\lambda_i = 2\pi \sqrt{\frac{2B}{|v_i|}} \quad (13)$$

Where h_0 is surface height at zero time, λ_i is the ripple wavelength in the x or y directions.

By changing the incident angle, ion flux, ion energy, and ion species, the magnitude of (v_x, v_y) will be changed, consequently the wavelength of ripples that induced on the solid surface will be changed.

Result and Discussion

A. Incident angle

Fig.2 Shows analytical solution for surface height using BH equation of silicon bombarded with Ar^+ ion at incident angles (a) 55° and (b) 85° off-normal..

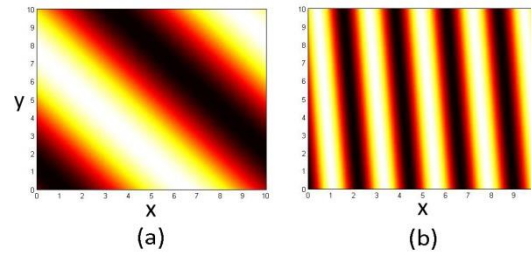


Fig.(2) Surface height of silicon bombarded by Ar^+ ion with energy 250eV, flux= $3.2 \times 10^{16}/\text{cm}^2$ s, arbitrary thermal diffusion coefficient (B)= $1 \text{ nm}^4/\text{s}$, and incident angle 55° (a) and 85° (b).

Analytical solution shows that the orientation of the created ripples or wave-like pattern of the surface is depending on the incident angle of incoming ions with respect to surface normal, the wave vector of ripples with wavelength is aligned parallel to the projection of the ion beam for angle of 55° off-normal on the irradiated surface. By further increasing of the incident angle to 85° off-normal, the ripples rotation have been observed.

For oblique angle, less penetration and higher sputtering have been observed which indicate that the upper layers near the surface participate in surface evolution and the driving force of the redeposit atoms along the ion beam direction increased and the ripple follow the ion beam projection, but for angles less

than critical for example at 55° , the sputtering yield is smaller and the penetration is higher which induce the redistribution of the target atoms which defected and perturbed due ion bombarding at the same time the driving force of the redeposited atoms on the surface has less range of motion. The cooperation between both effects could produce wave motion of the surface atoms normal to the ion beam projection.

These results are similar to the experimental results of Charbel Said Madi [24], as well as to results of the silicon surface irradiated at room temperature by 250eV Ar^+ ion at various incidence angle. Notably, at incidence angle 55° off-normal parallel mode ripples and angle 85° perpendicular mode ripples wave vector appeared with the ion beam projection.

B. Ion Flux

The ripple pattern, in particular its wavelength, depends also on the ion flux, J_{ion} , i.e., the number of incoming ions per area and time units. The ripple wavelength is very sensitive to parameters such as ion flux and temperature. These dependences mainly originate from both the relaxation process and concentration of the mobile defects on the surface.

Erlebacher, *et al* [19], for silicon surface bombarded by 0.75keV Argon ion at 67.5° to normal in the 500-600°C range, they reported that the ripple wavelength was decrease with ion flux, as $\lambda \sim J^{-1/2}$. Also a decrease of the ripple wavelength was reported for silicon surface irradiated by 1keV O_2^+ beam at incident angle of 52° , where in this case the quantitative dependent was not addressed [25]. Analytical solution for BH equation for the imaginary part of surface height of silicon bombarded by Ar^+ ion with energy (2keV) at incident angle of 67.5° , shows the ripple wavelength inversly dependence on the flux, as shown in Fig.3.

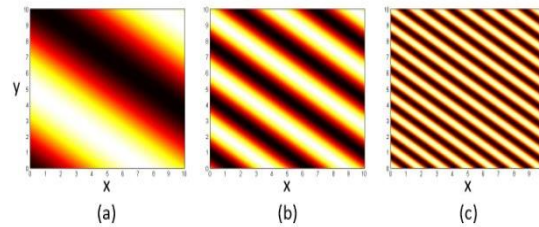


Fig.

3 Surface height of silicon bombarded by Ar^+ ion with energy 2keV, arbitrary thermal diffusion coefficient $(B)=0.1 \text{ nm}^4/\text{s}$, incident angle 67.5° , and flux (a) $1*10^{16}/\text{cm}^2.\text{s}$, (b) $1*10^{17}/\text{cm}^2.\text{s}$, and (c) $1*10^{18}/\text{cm}^2.\text{s}$.

C. Ion species

Different ion species can induce various morphology on targets of the same material and the wavelength of the wavelike pattern that form on the target surface for different ion species. Fig.4 shows the analytical solution of BH model for ripple formation on silicon surface irradiated by different ions (He, Ne, Ar, Kr, and Xe) with 8 keV at an incidence angle of 60° . It shows that the ripple wavelength is small for heavier incident ion (Xe) than that of the lighter ion (He).

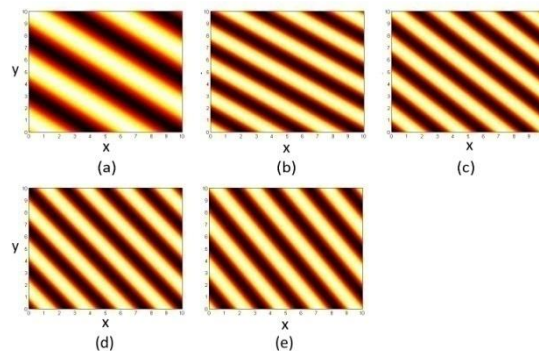


Fig.

4 Surface height of silicon bombarded by ions (a) He (b) Ne (c) Ar (d) Kr and (e) Xe with energy 8keV, arbitrary thermal diffusion coefficient $(B)=10 \text{ nm}^4/\text{s}$, incident angle 60° , and flux $1*10^{18}/\text{cm}^2.\text{s}$.

The same behavior was found by Ziberi *et al* [26], for Si irradiated with Ar^+ , Kr^+ , and Xe^+ ions at incident angle 15° with ion energy 500-

2000eV range. Bhattacharjee, *et al* [18], concluded that the ripple wavelength varies inversely with the mass of the incident ions, for Si target bombarded at an incidence angle of 60° with 8keV He^+ , N^+ , O^+ , and Ar^+ ions.

D. Ion Energy

The ion energy is an adjustable parameter of central importance in quantifying the ripple formation of various substrates [6].

Figure (5) shows the effect of different incident ion energies (250, 750, & 1200) eV of Ar^+ ion by an incident angle 60° , on Silicon surface, the result indicate that the ripple wavelength decrease with increasing incident ion energy. Similar trend have been observed by Brown [27], when they investigated the ion beam erosion-induced ripple formation on Si surface that irradiated by Ar^+ ion at incidence angle of 60° from the surface normal, temperature 990 K and fluence 7.2×10^{19} ions/cm². The ripple wavelength decreased from 740 nm to 350 nm with an increase in ion energy from 0.25 keV to 1.2 keV following a nearly inverse square dependence on ion energy in Bradley Harper theory.

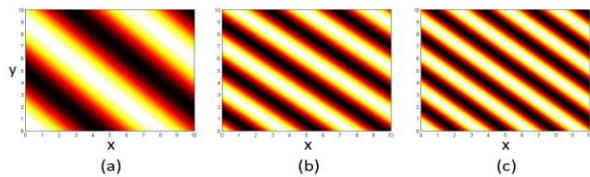


Fig.(5) Surface height of silicon bombarded by Ar^+ ion with flux 7.2×10^{18} /cm².s, arbitrary thermal diffusion coefficient (B)= 100 nm⁴/s, incident angle 60° , and incident ion energy (a) 250 eV , (b) 750 eV, and (c) 1200 eV.

In contract, some research groups observed a linear energy dependence of the ripple wave length; for silicon surface by Ar^+ bombardment at 60° incident angle in the ion energy range 50-140keV [7]. Also for silicon surface irradiated with Ar^+ , Kr^+ , and Xe^+ ions at angle 15° in the energy range 400-2000eV

[26]. These inconsistent in the results can be attributed to the thermal diffusion, if thermally activated surface diffusion is the dominant process for surface smoothing, the wavelength dependence on energy of bombardment is given by $\lambda \sim E^{-1/2}$. On the other hand in the absence of thermal diffusion, ion-induced effective surface diffusion becomes dominating contributor in thermal diffusion coefficient and it expected the energy dependence as $\lambda \sim E$ [17].

E. Thermal diffusion coefficient

The wavelength is found to increase with diffusivity as discussed by Bradley and Harper [8]. Bradley and Harper suggest, based upon a linear instability theory that the dominant wavelength should scale according to equation (1).

In our simulation we reported that the wavelength increases by increasing thermal surface diffusion coefficient as shown in Fig. 6.

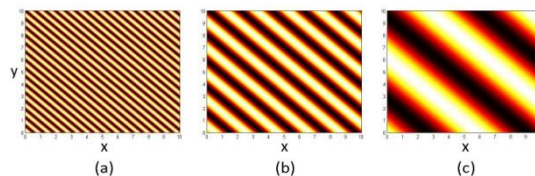


Fig.(6) Surface height of silicon bombarded by Ar^+ ion with energy 500eV, flux 2.87×10^{16} /cm².s at incidence angle of 15° , and arbitrary thermal diffusion coefficient, B, (a) 0.01 nm⁴/s, (b) 0.1 nm⁴/s, and (c) 1 nm⁴/s.

Similar result is found by Das [20], for different thermal diffusion coefficient (2×10^{-48} , 2×10^{-47} , and 2×10^{-46} m⁴/s) at angle 15° and fluence 2.87×10^{17} ions/cm² of argon ion that irradiated Silicon.

Conclusion

Analytical solution of Si surface modification by different ions based on the BH model shows the variance of wavelength of produced ripples or wavelike pattern with

incident angle, incident ion energy and flux, ion species and thermal diffusion coefficient.

The ripples on the silicon target surface that irradiated by Ar^+ ion oriented with incident angle, it is perpendicular or parallel to the ion beam projection on the target surface at an angles of 55° and 85° , respectively. The ripple wavelength decreases with increasing ion flux and ion energy.

Ion species affect on the wavelength of the ripple induced on the silicon surface. The

wavelength is small for heavier incident ion (Xe) than that of the lighter ion (He). Finally, the thermal diffusion coefficient, B, affected on the ripple wavelength, as B increase λ increased.

Acknowledgments

The Authers acknowledge the Faculty of Science and Educational Science, department of physics for supporting our work.

References

- [1]. Behrisch, Rainer, and Wolfgang Eckstein (1981) *Sputtering by Particle Bombardment I*, Springer-Verlag Berlin Heidelberg.
- [2]. Wasa, K., Makoto K. and Hideaki A. (2004) *Thin film Materials Technology Sputtering of Compound materials*, William Andrew, Inc.
- [3]. Wang, Y., Yoon S.F., Ngo C.y., and Ahn J. (2007)"Surface morphology evolution of GaAs by low energy ion sputtering", *Nanoscale Research Letters* 2: 504-508.
- [4]. Sanchez-Garcia, J. A., Gago R., Caillard R., Redondo-Cubero A., Martin-Gago J.A., Palomares F.J., Fernandez M., and Vazquez L. (2009) "Production of nanohole/nanodot patterns on Si (001) by ion beam sputtering with simultaneous metal incorporation", *Journal of Physics: Condensed Matter* 21: 224009.
- [5]. Zhao, Guiping (2007) "Fabrication and characterization of nanowire arrays on InP (100) surfaces", *Ph.D. dissertation*, Newcastle University, England.
- [6]. Zhou, Hua (2007) " Ion Beam Erosion-Induced Self-organized Nanostructures on Sapphire", *Ph.D. disseration*, University of Vermont, United State.
- [7]. Chini, T.K., Okuyama F., Tanemura M., and Nordlund K. (2003) "Structural investigation of keV Ar-ion-induced surface ripples in Si by cross-sectional transmission electron microscopy", *Physical Review B* 67: 205403.
- [8]. Bradley, R. and James M.E. Harper (1988)" Theory of ripple topography induced by ion bombardment", *Vacuum Science and Technology A* 6: 2390-2395.
- [9]. Zhou, Hua, Yiping Wang, Lan Zhou, Randall Headrick L., Ahmet S. Ozcan, Yiyi Wang, Gozde Ozaydin, Karl F. Ludwig, Jr., D. Peter Siddons (2007) "Wavelength tunability of ion-bombardment-induced ripples on sapphire", *Physical Review B* 75: 155416.
- [10]. Park, S., Kahng B., Jeong H., and Barabasi A.-L. (1999) "Dynamics of ripple formation in sputter erosion: nonlinear phenomena", *Physical review letters* 83: 3486.
- [11]. Cuerno, Rodolfo and Albert-Laszlo Barabasi (1995) "Dynamic scaling of ion-sputtered surfaces", *Physical review letters* 74: 4746.
- [12]. Makeev, Maxim A., and Rodolfo C., and Albert-Laszlo Barabasi (2002) "Morphology of ion-sputtered surfaces", *Nuclear Instruments and Methods in Physics Research Section B* 197: 185-227.

-
- [13]. Javier, Munoz-Garca, Mario C., and Rodolfo C., (2006) "Nonlinear ripple dynamics on amorphous surfaces patterned by ion beam sputtering", *Physical review letters* 96: 086101.
- [14]. Sigmund P., (1969) "Theory of sputtering. I. Sputtering yield of amorphous and polycrystalline targets", *Physical review* 184: 383.
- [15]. Liedke, Bartosz (2011) "Ion beam processing of surfaces and interfaces –Modeling and atomistic simulations-", *Ph.D. dissertation*, Dresden University of Technology, German.
- [16]. Hartmann, Alexander K.m and Reiner K., and Taha Y. (2009) "Simulating discrete models of pattern formation by ion beam sputtering", *Journal of Physics: Condensed Matter* 21: 224015.
- [17]. Chini, T.K., Sanyal M.K., and Bhattacharyya S.R. (2002) "Energy dependent wavelength of the ion induced nanoscale ripple", *Physical Review B* 66: 153404.
- [18]. Bhattacharjee, S., Karmakar P., and Chakrabarti A., (2012) "Key factors of ion induced nanopatterning", *Nuclear Instruments and Methods in Physics Research Section B: Beam Interactions with Materials and Atoms* 278: 58-62.
- [19]. Erlebacher, Jonah., Michael J., Eric C., Michael B., and Jerrold A. (1999) "Spontaneous pattern formation on ion bombarded Si (001)", *Physical review letters* 82: 2330.
- [20]. Das, Kallol (2010) 'Effect of irradiation parameters on the surface pattern evolution in silicon due to ion bombardment", *M.Sc. thesis*, University of Illinois, Urbana-Champaign.
- [21]. Keller, Adrian, Rodolfo Cuerno, Stefan Facsko, and Wolfhard Moller (2009) "Anisotropic scaling of ripple morphologies on high-fluence sputtered silicon", *Physical Review B* 79: 115437.
- [22]. Fulga, Florin, and Dan V. Nicolau (2010) "Simulation of the nanostructuring of surfaces under ion-beam bombardment", *Microelectronic Engineering* 87: 1455-1457.
- [23]. Marina, Ines Cornejo (2011) "Pattern Formation on Si surfaces by low-energy ion beam erosion", *Ph.D. dissertation*, university of Saarlandes, Saarbrucken/ Leipaig.
- [24]. Madi, Charbel Said (2011) "Linear stability and instability patterns in ion bombarded silicon surfaces", *Ph.D dissertation*, Harvard University, Cambridge, Massachusetts.
- [25]. Liu, Z.X., and P.F.A. Alkemade (2001) "Flux dependence of oxygen-beam-induced ripple growth on silicon", *Applied Physics Letters* 79: 4334-4336.
- [26]. Ziberi, B., F. Frost, Th. Hoche, and B. Rauschenbach (2005) "Ripple pattern formation on silicon surfaces by low-energy ion-beam erosion: Experiment and theory", *Physical Review B* 72: 235310.
- [27]. Brown, Ari-David (2005) "Studies of ion sputtered silicon (111) surfaces", *Ph.D dissertation*, Johns Hopkins University, Baltimore, Maryland.